

# Theory and Modeling of Stereoselective Organic Reactions

KENDALL N. HOUK, MICHAEL N. PADDON-ROW, NELSON G. RONDAN,  
YUN-DONG WU, FRANK K. BROWN, DAVID C. SPELLMEYER, JAMES T. METZ,  
YI LI, RICHARD J. LONCHARICH

Theoretical investigations of the transition structures of additions and cycloadditions reveal details about the geometries of bond-forming processes that are not directly accessible by experiment. The conformational analysis of transition states has been developed from theoretical generalizations about the preferred angle of attack by reagents on multiple bonds and predictions of conformations with respect to partially formed bonds. Qualitative rules for the prediction of the stereochemistries of organic reactions have been devised, and semi-empirical computational models have also been developed to predict the stereoselectivities of reactions of large organic molecules, such as nucleophilic additions to carbonyls, electrophilic hydroborations and cycloadditions, and intramolecular radical additions and cycloadditions.

A VERITABLE CORNUCOPIA OF SYNTHETIC METHODS FOR introducing molecular functionality with control of diastereoselectivity or enantioselectivity has been created (1). Synthetic organic chemists continue to devise methods to control stereoselectivity, so that stereogenic (2) centers in natural products or other synthetic targets may be introduced with great economy. We have studied stereoselective organic reactions with theoretical methods to understand how stereoselectivity arises, to predict stereoselectivities of new reactions, and to learn how to design new stereoselective processes.

Figure 1 shows several types of stereoselective reactions. In Fig. 1A, a classic example of a stereoselective reaction is given (3). The chirality of the organic substrate causes the new stereogenic center produced in the reaction to be formed with a predominance of one configuration. Although only modest stereoselectivity is found (4), Prelog showed that the direction of addition is predictable according to a simple steric model, now known as Prelog's rule (3). Figure 1B is an intramolecular Diels-Alder reaction of an achiral reactant to produce a product with four new stereogenic centers in a specific relative arrangement (5). Figure 1C shows an asymmetric hydrobor-

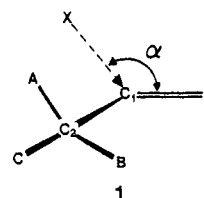
ation-oxidation reaction in which an optically active alcohol is formed from an achiral starting alkene by reaction with an optically active reagent (6). Interest in the development of optically active reagents and catalysts is extremely high. The Sharpless oxidation of allylic alcohols, shown in Fig. 1D, has become the paradigm of such a catalytic process (7).

The understanding and prediction of stereoselectivities are delicate matters. A difference of only  $1.8 \text{ kcal mol}^{-1}$  between the free energies of activation of two stereoisomeric transition states will give products in a ratio of 96.4 at  $25^\circ\text{C}$ ; a difference of more than  $2.8 \text{ kcal mol}^{-1}$  will give a preference greater than 100:1. Because the accurate calculation of such small differences in energy is a difficult challenge, quantitative formulations of stereoselectivity (8) and quantitative modeling of organic reactions (9) are rare.

To understand stereoselectivity, we must know the origins of subtle energy differences between stereoisomeric transition states. Our studies of stereoselectivity involve ab initio quantum mechanical predictions of the structures of transition states, rather than just of stable molecules, because "although one conformation of a molecule is more stable than other possible conformations, this does not mean that the molecule is compelled to react as if it were in this conformation or that it is rigidly fixed in any way" (10). The conformational analysis of transition states differs from conformational analysis of stable compounds because transition states cannot be observed; consequently, all information about them is either indirect or is obtained by theory. Transition states have several unusually long and weak bonds and abnormal bond angles, which may lead to unconventional conformational preferences. Systematic theoretical studies of transition structures have begun to elucidate the geometries of transition states and have led to models that are useful for predictions (11).

## Ab Initio Studies of Transition Structure Conformations

We have investigated the following aspects of addition transition structures, 1: (i) the angles of attack,  $\alpha$ , of reagents, X, upon multiple bonds; (ii) the rotational preferences about the  $\text{C}_1\text{-C}_2$



K. N. Houk is a professor in the Department of Chemistry and Biochemistry, University of California, Los Angeles 90024. N. G. Rondan is a research scientist at Dow Chemical Company, Midland, MI 48640. M. N. Paddon-Row is a professor at the University of New South Wales, Kensington, New South Wales 2033, Australia. Y.-D. Wu, F. K. Brown, D. C. Spellmeyer, J. T. Metz, Y. Li, and R. J. Loncharich are former graduate students in the Department of Chemistry, University of Pittsburgh, Pittsburgh, PA 15260, where the work described in this article was performed.

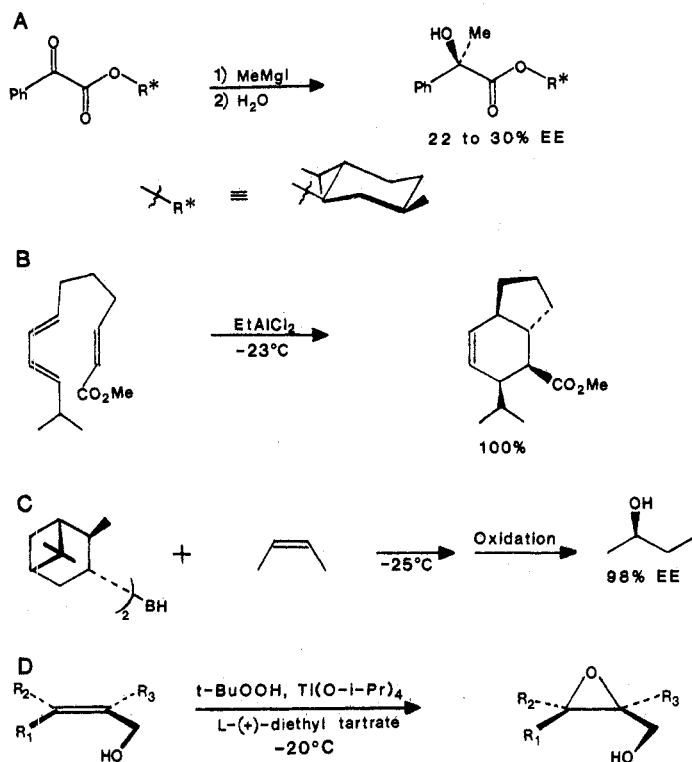


Fig. 1. Examples of stereoselective organic reactions.

bonds of transition structures; and (iii) the preferred locations of allylic substituents A, B, and C in the transition structures. If  $C_2$  is a stereogenic center (that is, if A, B, and C are different), and if one conformation of the allylic bonds is highly preferred, then there are six different ways to place A, B, and C on the allylic positions. Three of these correspond to attack on one face of the  $C=Y$  bond, and the remaining three correspond to attack on the opposite face. To predict the stereoselectivity of such a reaction, we must predict the relative energies of these six conformations with a high degree of accuracy (12).

## Attack Angles and Reactant Distortions in Addition Reactions

The preferred trajectory of attack on multiple bonds has been discussed many times (11, 13, 14). Our calculations focus on the transition structure attack angle,  $\alpha$ . We have not investigated the entire trajectory from reactants to products, since this will be kinetically irrelevant and will have no direct influence on product stereoselectivities.

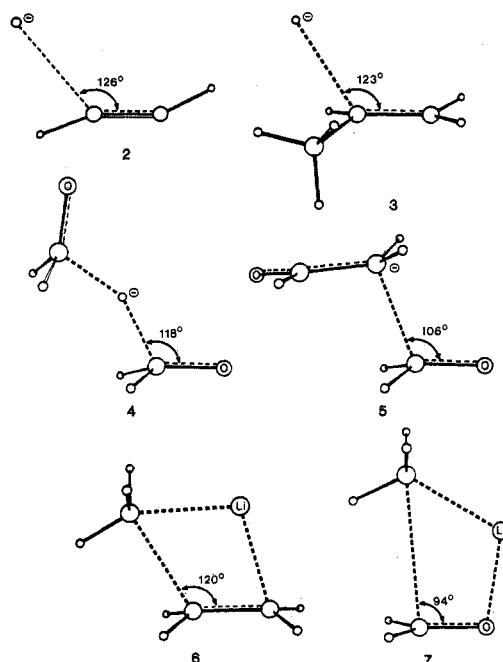
**Nucleophilic attack.** Qualitative considerations (13), model calculations (11, 13–15), and x-ray crystal structures of molecules containing amine and carbonyl groups in close proximity (16) suggest that nucleophiles attack carbonyls at approximately tetrahedral angles ( $109.5^\circ$ ). This angle may be relatively rigid or easily deformable (13, 15, 17).

Calculations on the reactions of simple charged nucleophiles, such as  $H^-$ , with carbonyl compounds in the gas phase show that these reactions usually have no barriers. The activation energies for these reactions in solution arise from desolvation of the nucleophile. However, there are barriers for the gas-phase reactions of nucleophiles with alkenes and acetylenes and for the reactions of stabilized

nucleophiles with carbonyl compounds, so that an investigation of angles of attack in these cases is possible.

Our ab initio quantum mechanical calculations were carried out with GAUSSIAN 80 and 82 (18), a series of computer programs for such studies developed by Pople and co-workers. The calculations that we perform use the 3-21G basis set, and in the cases where our calculations have been compared with more accurate ones, the qualitative conclusions described below survive. Some of the many transition states for nucleophilic additions calculated in our laboratories are summarized in structures 2 through 7, which are described below. In these and subsequent structures, the small unlabeled circles represent hydrogen atoms and the large unlabeled circles are carbons. All other atoms are labeled.

Charged nucleophiles react with alkenes or acetylenes with obtuse attack angles,  $\alpha$ , of  $115^\circ$  to  $130^\circ$ . Structures 2 and 3 are transition structures for the attack of hydride on acetylene and propene. The calculated force constants of the transition structures indicate that the deformation of  $\alpha$  from these values can occur about one-half as easily as the bending of a normal  $C-C-C$  or  $H-C-C$  angle (17). The angle of attack decreases as the  $\pi$  bond becomes more unsymmetrical, as in the  $C_{2v}$ -constrained hydride transfer from methoxide to

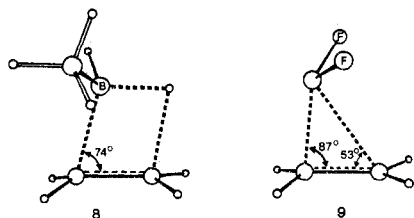


formaldehyde (structure 4) or the gas-phase aldol reaction of the enolate anion with formaldehyde (structure 5). The unsaturated electrophilic component in these reactions is always bent substantially toward a product geometry and, for alkenes and alkynes, in a *trans* fashion (19).

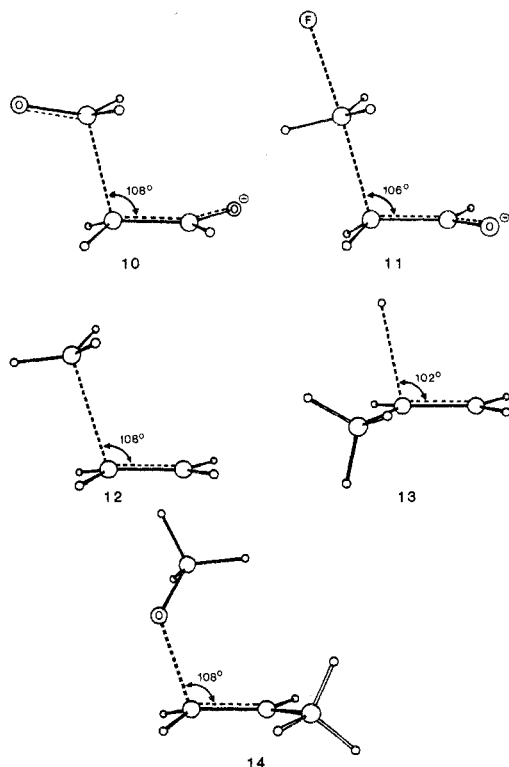
The additions of organolithium or metal hydride reagents occur through four-center transition structures (6 and 7) (20). The attack angle is smaller than that for charged nucleophiles because of the polarization of the multiple bond by metal coordination and the cyclic nature of the transition structure. The pattern of smaller  $\alpha$  for carbonyl reactions than for alkene reactions is observed in these organometallic reactions. In solution, these reactions may involve either cyclic or acyclic transition states and solvated or aggregated organometallics.

**Electrophilic attack.** The reactions of charged electrophiles with alkenes in the gas phase have no barriers, although differential solvation effects between reactants and transition structures give rise to activation barriers in solution. Neutral electrophiles react in the

gas phase via three- or four-center transition states (21). Studies of hydroborations (22) and carbene cycloadditions (23) show that, for electrophilic attack on multiple bonds, an acute angle of approach is favored, as shown in structures 8 and 9. Experimental evidence

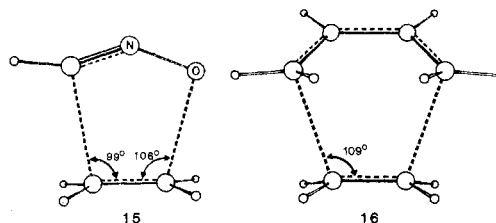


indicates that protonation in solution occurs through an acyclic intermediate; however, there is ample evidence for formation of cyclic ionic intermediates in brominations, mercurations, and related electrophilic additions, and these reactions must involve an acute angle of attack of the electrophile on the multiple bond. In the transition structures for electrophilic additions, the alkene C-C bond is stretched, but the geometry is otherwise relatively unperturbed. Thus, electrophilic attack on symmetrical alkenes or alkyl-ethylenes occur with acute  $\alpha$ 's and little pyramidalization of the unsaturated system. These features differ significantly from those described earlier for nucleophilic attack. When formaldehyde (structure 10) or methyl fluoride (structure 11) attack the enolate ion, which can be considered a very unsymmetrical alkene,  $\alpha$  becomes nearly tetrahedral.



**Radical attack.** In radical additions (structures 12 to 14), a nearly tetrahedral attack angle is favored (24, 25). There is little dependence of  $\alpha$  on the nature of the radical or alkene except that attack at a substituted carbon (structure 13) occurs with a slightly smaller angle than attack at an unsubstituted carbon (structures 12 and 14). The alkene distortion is intermediate between that calculated for nucleophilic and electrophilic attack. The ease of deformation of  $\alpha$  has been estimated to be approximately one-fourth that of the angle between normal single bonds (17).

**Pericyclic reactions.** Pericyclic reactions involve concerted bond formation. In examples such as the 1,3-dipolar cycloaddition of fulminic acid to ethylene (structure 15) and the Diels-Alder reaction of butadiene with ethylene (structure 16), nearly tetrahedral  $\alpha$ 's are predicted (26). The geometries of the alkenes and the values of  $\alpha$  for these pericyclic reactions are similar to those calculated for radical additions.



## A Frontier Molecular Orbital Model of Attack Angles

The variation in attack angles with changes in reagents and substrates can be understood qualitatively in terms of frontier molecular orbital (FMO) theory (27). According to FMO theory, the dominant stabilization of a transition state occurs by interaction of the highest occupied molecular orbital (HOMO) of one molecule with the lowest unoccupied molecular orbital (LUMO) of the other. This interaction causes the occupied orbital to be stabilized, which lowers the total electronic energy. The HOMO-LUMO interaction increases as the overlap between the orbitals increases and as the energy gap between these orbitals decreases. The HOMO and LUMO of ethylene are the  $\pi$  and  $\pi^*$  molecular orbitals, shown in the center of Fig. 2. The LUMO of the electrophile has been shown as a  $1s$  orbital, but it could just as well be a vacant  $p$  orbital of a borane or carbene or a low-lying  $\pi^*$  orbital of a dihalogen or peroxide. The stabilizing HOMO-LUMO interaction is maximized upon an acute angle of approach of the electrophile to ethylene, since this direction of approach maximizes the HOMO-LUMO overlap.

For attack of a nucleophile on a multiple bond, the important FMO interactions are shown at the right of Fig. 2. The HOMO interaction is destabilizing because both orbitals are occupied. Overlap and destabilization are maximized for an acute angle of approach. Destabilization is reduced when  $\alpha$  is obtuse, since this

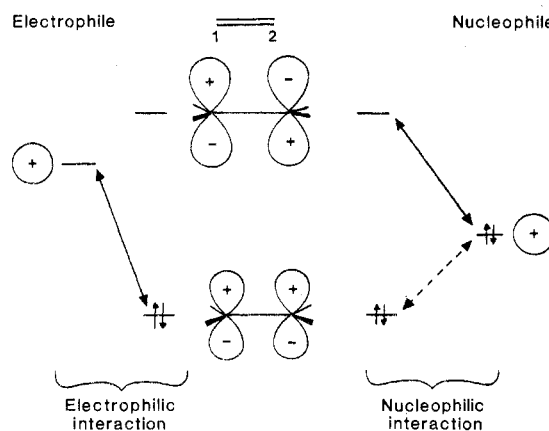
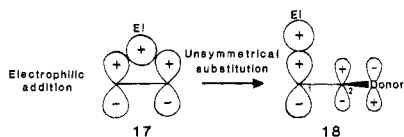


Fig. 2. Frontier molecular orbitals of an electrophile, ethylene, and a nucleophile, and interactions that occur in addition reaction transition structures.

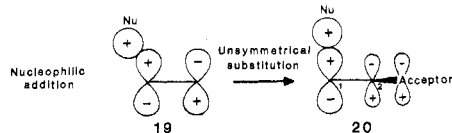
reduces the overlap between the two HOMO's. The stabilizing interaction between the nucleophile's HOMO and the alkene's LUMO is also maximized by an obtuse  $\alpha$ , since in this case the overlap integrals between the nucleophile HOMO and the  $p$  orbitals at  $C_1$  and  $C_2$  that make up the LUMO are of opposite sign.

Substituents alter these attack angles in a predictable way. Structure 17 shows the HOMO of a symmetrical alkene interacting with the LUMO of an electrophile. Placement of a donor substituent at one alkene terminus causes admixture of the donor orbital into the  $\pi$  molecular orbital in an antibonding fashion and distortion of the HOMO in the sense shown in structure 18. The attack angle will



therefore increase to maximize overlap of the electrophile LUMO at the site of the alkene with the larger coefficient. For a very potent donor, an  $\alpha$  of  $90^\circ$  is expected. However, since the site being attacked will also pyramidalize, a limiting angle of  $109.5^\circ$  is expected for unsymmetrical alkenes. The attack of formaldehyde (structure 10) or methyl fluoride (structure 11) on the enolate ion, one of the most unsymmetrical alkenes, are examples of this.

Nucleophilic attack on a symmetrical alkene occurs with a larger  $\alpha$  than attack on a carbonyl group. As shown by the transformation of structure 19 to 20, an acceptor substituent or the electronegative



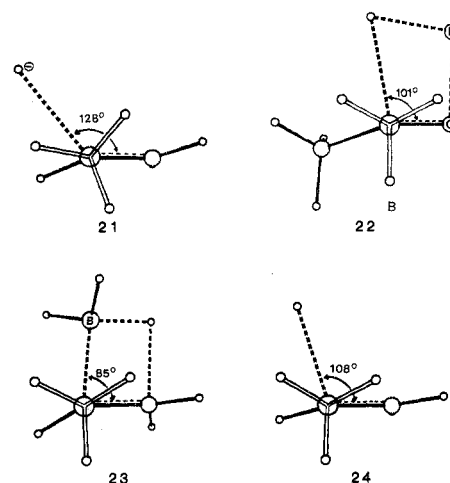
oxygen terminus of a carbonyl makes the coefficient of  $C_1$  in the  $\pi^*$  molecular orbital larger than that of the substituted terminus or of a carbonyl oxygen. Since pyramidalization also occurs, the attack angle should approach  $109.5^\circ$  for an unsymmetrical electrophilic  $\pi$  system. Thus, attack angles on carbonyls are smaller than those on alkenes, and complexation of a carbonyl oxygen by a Lewis acid catalyst should further reduce  $\alpha$ .

## Substituent Conformations in Transition States

Our calculations have revealed some unexpected features about how substituent conformations respond to the unnatural bond lengths and angles in transition states. We first consider conformations about forming C-C bonds. In 12, the transition structure for the attack of a methyl radical on ethylene is shown. There is perfect staggering of the methyl group with respect to the bonds to the alkene terminus. The corresponding transition structure with an eclipsed conformation is calculated to be  $0.5 \text{ kcal mol}^{-1}$  higher in energy. Similarly, for the addition of methyl anion or methyl lithium to ethylene (structure 7), the staggered transition structures are favored over the eclipsed ones by  $0.2 \text{ kcal mol}^{-1}$ . For the aldol reaction (10) and methyl fluoride attack on enolate (11), the staggered arrangement around the forming bond is preferred. For the usual values of C-C bond lengths in transition structures (30 to 60 percent stretched), barriers about forming bonds are expected to be between 1.8 and  $0.2 \text{ kcal mol}^{-1}$ . For relatively late transition structures with nearly completely formed bonds, the barriers are

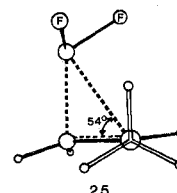
sufficiently high to ensure primarily staggered transition structures, whereas very early ones should be quite easily distorted to eclipsed when steric constraints promote such an arrangement. Some cyclic transition structures, such as those of hydroborations and carbene cycloadditions, are necessarily eclipsed about the forming bonds.

Calculations have also been performed to assess the conformational preferences with respect to single bonds attached to atoms undergoing bonding changes in transition structures (11, 17, 28). Transition structures 3, 8, and 13, described earlier show that the methyl groups attached to atoms involved in bonding changes are staggered with respect to the forming bond and to the remaining two bonds to the atom being attacked. Newman projections looking along the C-C bond from the methyl carbon toward the carbon being attacked by the reagent are shown for two nucleophilic additions in structures 21 (hydride plus propene) and 22 (LiH plus acetone). Each projection also shows  $\alpha_p$ , the angle of attack projected onto a plane perpendicular to the bond from the methyl group to the atom being attacked. The corresponding angle will be approximately  $120^\circ$  in each reaction product. Similar projections for an electrophilic and a radical addition are shown in structures 23 and 24. The information in these drawings can be summarized as



follows: the methyl C-H bonds prefer a staggered arrangement with respect to the partially formed bond. Nucleophilic attack leads to the largest  $\alpha_p$  and to the greatest pyramidalization of the carbon being attacked. The allylic methyl C-H bonds are nearly perfectly staggered in nucleophilic transition structures. This conclusion was reached empirically by Felkin in 1968 (29) and has been supported computationally by Anh (11) for nucleophilic additions. Our group has extended this conclusion to all types of additions (17, 28). Computational estimates show that rotational barriers involving torsional interactions with partially formed bonds may be as large ( $\sim 3 \text{ kcal mol}^{-1}$ ) as those involving fully formed bonds (17).

Upon radical attack (structure 24), pyramidalization of the carbon under attack is small, perfect staggering is not possible, and the rotational barrier is now only  $2 \text{ kcal mol}^{-1}$ . For electrophilic reactions, such as hydroborations, the barriers to rotation about the C-B or C-C bond are about  $3 \text{ kcal mol}^{-1}$ . For a very acute angle of approach, as in carbene cycloadditions (structure 25), the preferred



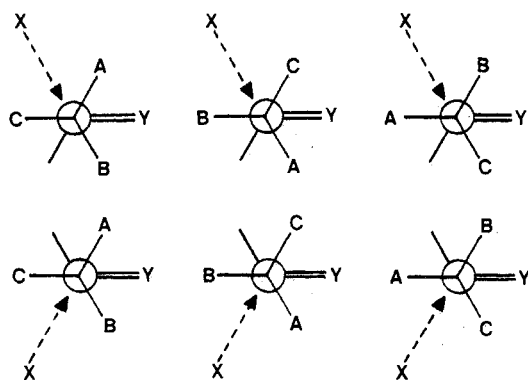


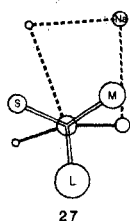
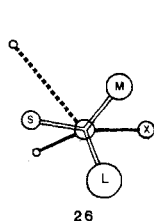
Fig. 3. Six staggered transition structures for attack of a reagent on a chiral unsaturated molecule.

conformation of the allylic group in the transition structure is only slightly different from that of the alkene ground state.

Our results show that conformations of substituents in transition structures may be quite different from those in the reactants. Alkenes or carbonyls have one allylic bond eclipsed with the double bond in the ground state, but the transition structure conformations are more product-like. Rotational barriers involving torsional interactions with partially formed bonds are nearly as large as those involving fully formed bonds. Consequently, the assumption of staggering in transition states is just as reasonable as the assumption of staggering in stable molecules. Thus, as shown in the Newman projections in Fig. 3, the attack of a reagent, X, on an unsaturated molecule with an allylic chiral center can occur from any of six possible staggered conformations. Nonstaggered conformations can be safely assumed to be higher in energy. The first three conformations all involve attack of the reagent from the top face and lead to one diastereomeric product, and the last three give the other diastereomeric product. Experimental results show which diastereomer is favored but give no direct information about which of the staggered transition structures is lowest in energy. Theoretical studies, complemented by experimental studies (30–32), have led to generalizations about which of the six transition structures shown in Fig. 3 are favored in particular cases.

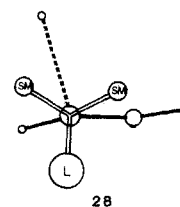
### Conformational Preferences of Allylic Groups in Transition Structures

**Steric effects.** When an allylic chiral center bears three groups of different size but not of greatly different electronic character, the preferred product arises from the transition state that has the largest group in the least crowded position and the smallest group in the most crowded position. For several reactions, we have determined the preferred arrangement by model *ab initio* or force-field calculations (the latter is discussed below), in which allylic hydrogens are replaced by alkyl groups and the energies of different conformations of the transition state are calculated. Structures 26 and 27 summarize preferred steric models for two nucleophilic additions. Newman projections with differently sized allylic groups in their preferred

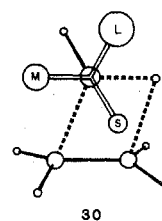
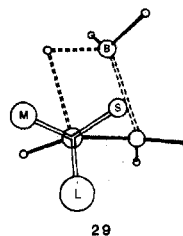


locations are shown. For nucleophilic additions with very obtuse angles of approaching (structure 26), there is a great preference for the conformation that has the largest group (*L*) *anti* to the attacking nucleophile, the medium-sized group (*M*) inside (near the double bond), and the smallest group (*S*) outside (away from the double bond) in the crowded region between the substituent (or H) on the double bond and the approaching nucleophile. These structures illustrate the Felkin-Anh model of asymmetric induction in nucleophilic additions to chiral carbonyl compounds (11, 29) modified by the obtuse angle of approach of the nucleophile and the pyramidalization of the carbon being attacked (11, 13, 17). This model shows why a small group favors the outside position and why the replacement of an aldehyde hydrogen by an alkyl group increases chiral crowding and thus enhances stereoselectivity. This model predicts the same major product as is predicted by Cram's Rule, an empirical rule proposed in 1952 (33).

As the attack angle  $\alpha$  decreases, the difference between crowding of inside and outside positions decreases. Thus, the nucleophilic attack on carbonyls via cyclic four-centered transition structures (27) should be less stereoselective than those proceeding through acyclic transition states (for example, structure 26). For radical additions, no stereoselectivity is predicted from model calculations unless there is a bulky group *cis* to the chiral center (structure 28). In such a case, the preferred location of substituents is as follows: *L*,

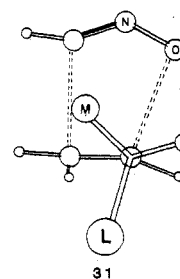


*anti*; *M*, out; *S*, in. Hydroborations follow such an "inside-crowded" model for chiral centers on either carbon (structure 29) or boron (structure 30). The resulting stereochemistry is sometimes



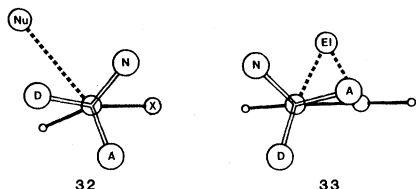
referred to as "anti-Cram" because it is opposite to the stereochemistry predicted by Cram's rule for nucleophilic additions. This "inside-crowded" or "anti-Cram" preference is also observed experimentally for enolate alkylations (31) and will hold whenever the inside position is more crowded than the outside.

There is another family of electrophilic additions, such as nitrile oxide cycloadditions (structure 31), in which the outside position is



more crowded than the inside. This "outside-crowded" model correctly predicts the preferred products of nitrile oxide cycloadditions (34), hexachlorocyclopentadiene Diels-Alder reactions (35), and osmium tetroxide hydroxylations (32), and it will probably prove to be general for addition and cycloaddition reactions with five- and six-membered transition states (34).

**Electronic effects.** When allylic substituents are either electronegative or electropositive relative to hydrogen, electronic effects cause these substituents to orient in a specific fashion with respect to the attacking reagent. On the basis of model calculations (11, 22, 30), the generalizations shown in structures 32 and 33 can be made. For



nucleophilic attack on  $\pi$  bonds, electronegative allylic groups (*A*, for acceptors) prefer the *anti* conformation so that the withdrawal of electrons from the  $\pi$  system can be maximized. The most electropositive group will prefer to be outside to minimize the donation of electrons to the perturbed  $\pi$  system of the already electron-rich transition state. Figure 4 shows why this occurs. When the  $\sigma_{C-A}^*$  orbital is aligned *anti* to the forming bond, its overlap with the HOMO of the transition state, consisting of a mixture of the nucleophile HOMO and the carbonyl LUMO, is maximized. This overlap of the substituent LUMO with the transition structure HOMO results in stabilization. Overlap and stabilization disappear when  $\sigma_{C-A}^*$  is perpendicular to the forming bond. When *A* is inside or outside, the  $\sigma_{C-A}^*$  orbital is gauche to the HOMO, overlap is relatively small, and stabilization is smaller. Electropositive groups (*D*) prefer the outside or inside positions because the interaction of an occupied  $\sigma_{C-D}$  orbital with the transition structure HOMO is destabilizing. This destabilization is maximized when  $\sigma_{C-D}$  is *anti* and is minimized when  $\sigma_{C-D}$  lies near the carbonyl plane, which occurs best when *D* is outside.

Electrophilic reactions show the opposite preference, as shown in structure 33 (30). The most electropositive allylic group should be *anti* to maximize electron donation from the high-lying  $\sigma_{C-D}$  orbital to the transition state LUMO, which consists of electrophile LUMO mixed with some alkene HOMO. The outside position is second best, and the donor avoids the inside position, where  $\sigma_{C-D}$  overlap with  $\pi^*$  will be negligible. Electronegative group *A* prefers the inside or outside positions. The interaction of  $\sigma_{C-A}^*$  with the transition state LUMO is not itself destabilizing, since both orbitals are vacant, but the overlap of  $\sigma_{C-A}^*$  with the alkene HOMO will stabilize the latter and decrease its interaction with the electrophile LUMO. In other words, C-A favors the inside or outside positions to minimize electron withdrawal by  $\sigma_{C-A}^*$  from the already electron-deficient transition state. Whether inside or outside is the best location for *A* depends on the specific dihedral angles as well as the interactions between the attacking electrophile and groups at the inside or outside positions.

Occasionally, steric and electronic factors predict opposite preferences. For example, in nucleophilic additions an electropositive trimethylsilyl substituent would prefer to be *anti* because of steric effects but outside because of electronic effects. In contrast, such a substituent should be preferentially *anti* in electrophilic additions for both steric and electronic reasons.

Another complicating feature is the possibility of additional factors such as coordination between a substituent and a reagent. For example, "chelation control" in nucleophilic additions to car-

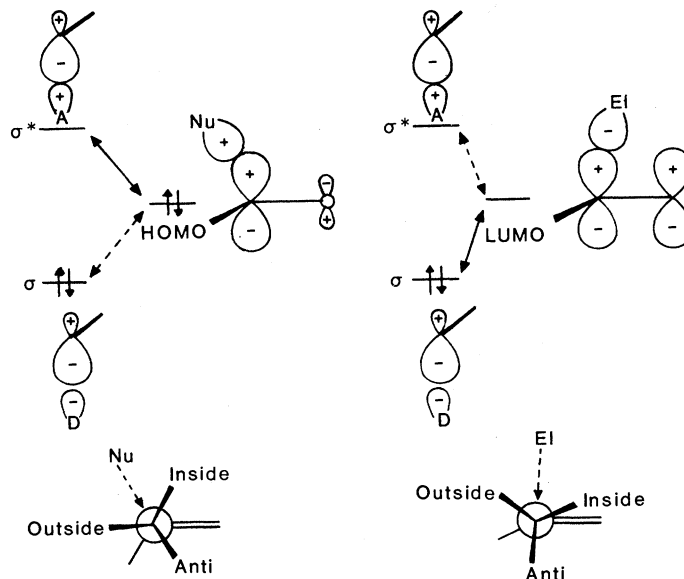
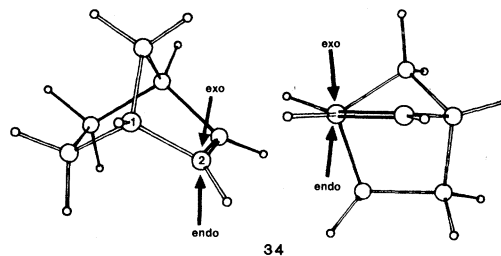


Fig. 4. Interactions of electronegative (*A*) and electropositive (*D*) allylic groups with the HOMO of a nucleophilic transition structure or LUMO of an electrophilic transition structure. Full arrows indicate stabilizing interactions, and dashed arrows indicate destabilizing interactions.

bonyl compounds occurs when allylic oxygens or nitrogens coordinate to a metal that is also coordinated to the carbonyl oxygen. Such chelation control will force the electronegative allylic substituent to occupy the inside position. Similarly, intramolecular reactions may permit the connecting chain to adopt only inside or outside conformations.

## Evidence for Staggering in Transition Structures of Addition Reactions

The proposal that staggering with respect to forming bonds always occurs in transition states of addition reactions is the cornerstone of the rules described in the preceding section. Is there experimental evidence to support this computational prediction? Norbornene and related molecules react stereoselectively from the *exo* face, as shown in the two views of 34, and with an unusual

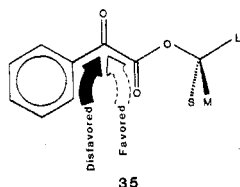


facility that cannot be accounted for in terms of strain effects alone (36). However, both *exo* stereoselectivity and the enhanced reactivity displayed by norbornene can be rationalized in terms of the tendency toward maximum staggering of the allylic bonds with respect to those attached to the reaction site in the transition state (28, 37). *Exo* attack involves a nicely staggered arrangement about the C<sub>1</sub>-C<sub>2</sub> bond. In contrast, *endo* attack involves a more nearly eclipsed arrangement. An activation energy difference of as much as 6 kcal mol<sup>-1</sup> could be achieved in a cycloaddition that occurs with perfect staggering compared to a hypothetical case involving perfect eclipsing.

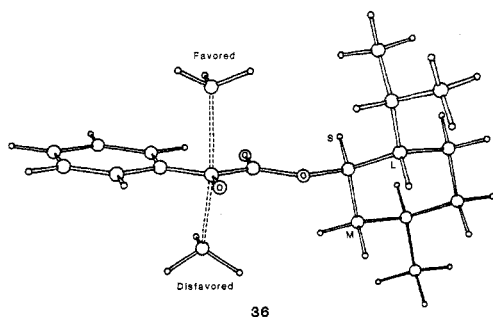
## Modeling Stereospecific Organic Reactions

The qualitative models described above, like the manipulation of molecular models, often provide satisfying rationalizations of experimental results, but quantitative predictions cannot be made on either basis. Real reactions may have idiosyncrasies not accounted for by qualitative general rules. There is a rule to cover all possible experimental outcomes, but predictions are often very difficult to make. To remedy this situation, we have begun to develop numerical computational models that keep track of the many factors that can influence stereoselectivities and that will predict the stereoselectivities of complex reactions. The *ab initio* calculations described earlier cannot be applied directly to the examples such as those shown in Fig. 1 because of the enormous computer time required for such calculations (38). A much faster technique is required to deal with large systems. Our computational models are based on Burkert and Allinger's MM2 method (39), a force-field technique that has been parameterized and tested for stable molecules that incorporate many common functional groups. Our models incorporate equilibrium bond lengths and angles from *ab initio* transition structure calculations for those bonds that are forming or breaking in the reaction. In rigid versions of our model, the positions of the atoms involved in bonding changes are fixed, regardless of the substituents. In the flexible models, the positions of all atoms are optimized with a force-field consisting of MM2 parameters for normal atoms and new parameters that we have developed for atoms involved in bonding changes.

**1,4-Asymmetric induction. Prelog's rule.** Prelog's rule (3) is an empirical model used to predict the major product of reactions of phenylglyoxylates with nucleophiles. When the reactant is arranged as in structure 35, the major product arises from attack of the



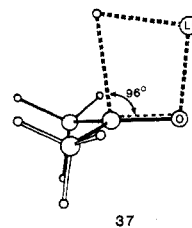
nucleophile near the side of *S*, not *M*. From model *ab initio* calculations, we obtained an approximate transition structure for methyl anion attack on glyoxylic acid. We then created a rigid model, fixing the position of the carbon of the nucleophile ( $\text{CH}_3^-$ ) and the atoms of the phenylglyoxylate moiety. The geometry of the chiral auxiliary, the (-)-menthyl group, and the  $\text{CH}_3^-$  hydrogens, are fully optimized for attack of  $\text{CH}_3^-$  from the top or bottom face. Structure 36 shows methyl anions approaching either face of (-)-



menthyl phenylglyoxylate. Although the optimized transition structures differ from each other in detail, the differences are almost imperceptible, so that this single diagram serves to show in detail why attack of the methyl anion on the top face is preferable. The

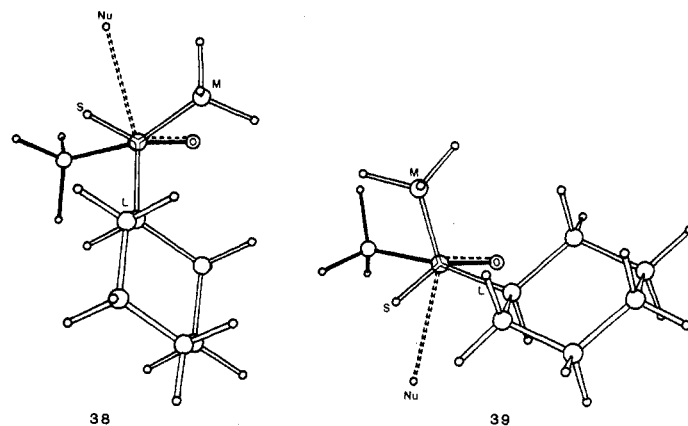
favored approach places the methyl anion near the smallest group (H) at the chiral center attached to oxygen, and the disfavored mode brings the methyl anion near the medium-sized group (*M*) of the cyclohexane. This particular conformation is anchored by the largest group, as suggested by Prelog's model. The calculations predict 24 percent stereoselectivity, whereas experimental results for methyl Grignard addition are 22 to 30 percent (1). Calculations that use this model for reactions with other homochiral auxiliaries give similarly good agreement with experiment.

**1,2-Asymmetric induction in nucleophilic additions.** Nucleophilic additions to carbonyls should be particularly difficult to model because of the influence of metal cation coordination and solvation on stereochemistry. Nevertheless, rather simple force-field (9) and steric congestion (40) models are surprisingly successful in accounting for the stereochemistries of hydride reductions of cyclic ketones. A rigid MM2 model that we have developed, based on structure 37



but with an  $\alpha$  of  $100^\circ$  and the metal cation removed, is quite adequate for semiquantitative predictions of stereoselectivity in sterically controlled nucleophilic additions to carbonyl compounds.

Structures 38 and 39 are the preferred transition structures for formation of the major and minor products of lithium aluminum hydride reduction of 3-cyclohexyl-2-butanone. There are eight other all-staggered transition state conformations for formation of each of the two diastereomeric products. Our stereoselectivity prediction comes from calculations of a Boltzmann distribution including all low-energy conformations. However, structures 38 and 39 differ in



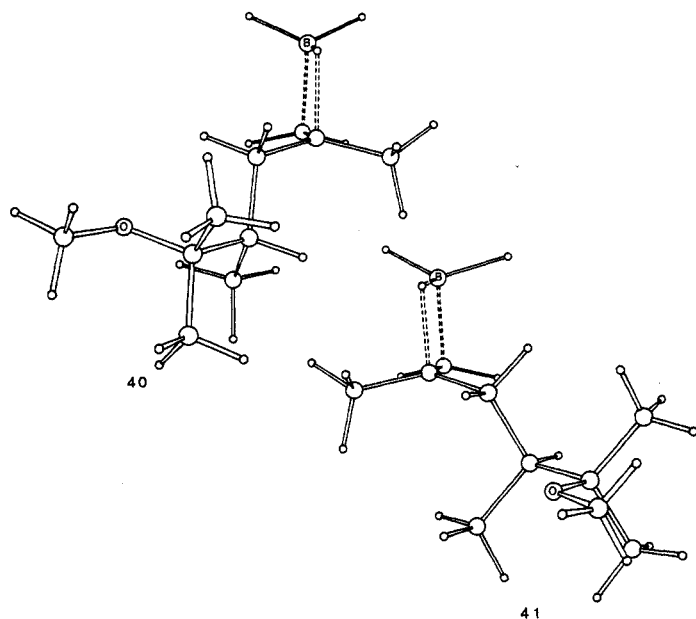
energy by  $0.6 \text{ kcal mol}^{-1}$ , and most of the 40 percent diastereomeric excess (DE) of the product from structure 38 that is predicted by our model arises from this difference. Experimentally, the  $\text{LiAlH}_4$  reduction gives a 1.6:1 ratio (24 percent DE) at  $35^\circ$ . This MM2 model has been applied to the series where the methyl group connected to the carbonyl in structure 38 or 39 is replaced by an ethyl, isopropyl, and *t*-butyl group. The experimental stereoselectivities are 33, 60, and 24 percent, respectively (29). Selectivities of 51, 64, and 62 percent are predicted by the MM2 model. There is moderate agreement, except that the large decrease in stereoselectivity for  $\text{R} = \text{Me}$  (methyl group) is not adequately predicted. As pointed out by Felkin (29) and as shown earlier in structures 26 and

27, the best arrangement of substituents is as follows: *L*, *anti*; *M*, in; *S*, out.

This model has also been applied to reduction of cyclohexanones, whose stereoselectivities have been the subject of a variety of empirical models (1, 40, 41). As shown in the two views of the transition structures for axial and equatorial attack on 3-methylcyclohexanone (Fig. 5), the preference for axial attack may be attributed to the smaller torsional interactions that occur upon axial attack (29). The ratio of axial to equatorial attack is 77:23 according to calculations, since the axial transition structure is 0.7 kcal mol<sup>-1</sup> more stable than the equatorial one. Ratios from 87:13 to 84:16 are found experimentally for LiAlH<sub>4</sub> or NaBH<sub>4</sub> reductions (1, 41). The model correctly predicts that a 3-axial substituent, as in 3,3,5-trimethylcyclohexanone, makes equatorial attack slightly favored due to the 1,3-diaxial interaction, which destabilizes axial attack.

**Electrophilic additions.** A notable difference between structures 26 or 27 and structure 29 is that nucleophilic additions to carbonyls (for example, with aluminum hydride or borohydride reducing agents) should give the opposite stereochemistry from that achieved with electrophilic borane reductions of carbonyls or of the corresponding alkenes. This prediction (17) has been verified by the experimental work of Midland and Kwon (42, 43).

Remote asymmetric induction can also be rationalized by an extension of such models to account for preferred conformations of groups far removed from the site of bonding changes. For example, Evans and co-workers reported significant 1,3-asymmetric induction in the hydroboration of alkenes (44). The MM2 models for the transition structures for formation of the major and minor products of this reaction (structures 40 and 41) show that the differentiation between these is due to the 1,3-dimethyl interaction, which destabi-



lizes structure 41, as proposed by Evans before our calculations (44). The calculated difference in energy between structures 40 and 41 is 0.8 kcal mol<sup>-1</sup>, which is in good accord with the approximately 80:20 ratio of diastereomers found in several reactions of this type (22, 44). The preference for the largest allylic group (LCHMe) to align *anti* to the forming C-H bond and the arrangement of the large group (*L*) *anti* to the C<sub>2</sub>-C<sub>3</sub> bond enforces these conformations.

Transition structures 42 to 45 are models used to rationalize the stereochemistries observed for electrophilic additions to a chiral allylic ether and an allylic alcohol. The nitrile oxide cycloaddition to a chiral allylic ether (structure 42) follows the rules described earlier,

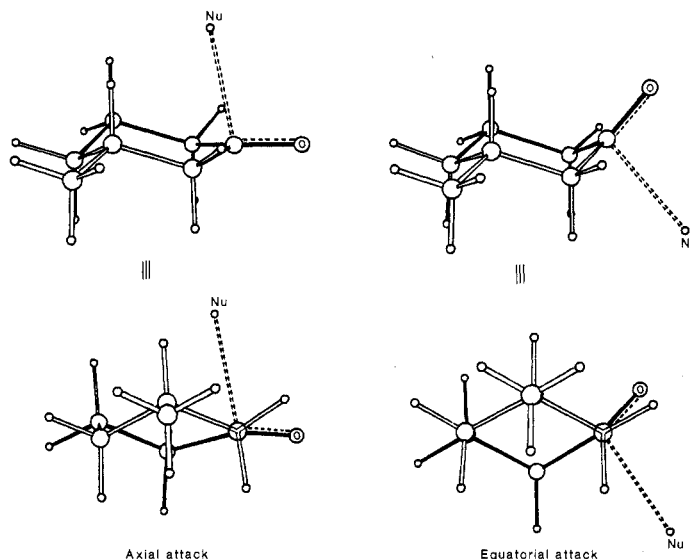
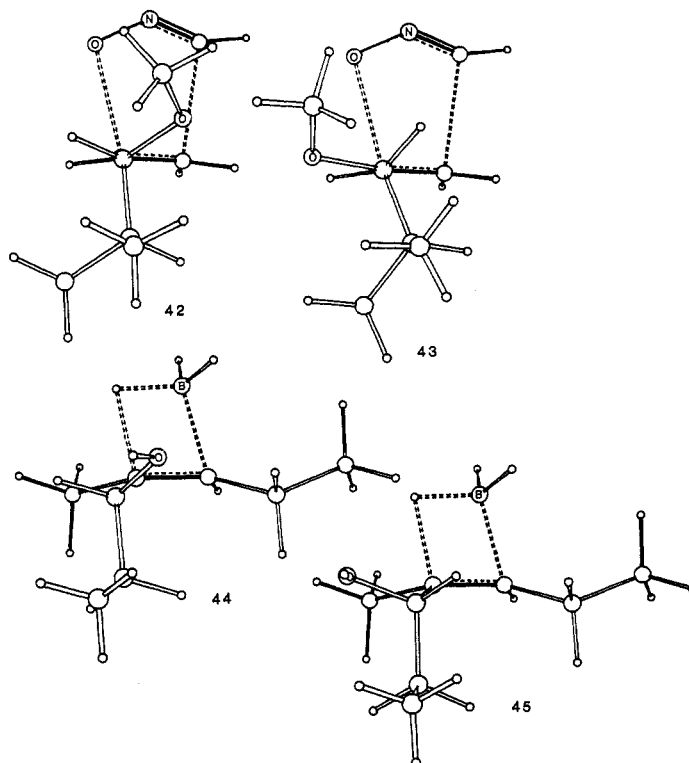


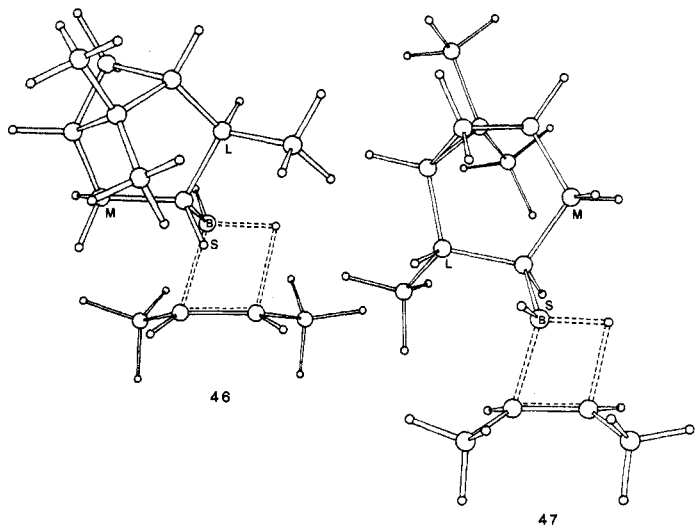
Fig. 5. MM2 transition structure models for the hydride (nucleophile, Nu) reduction of 3-methylcyclohexanone.

with the largest group *anti* and most electronegative group inside (30). The transition structure with the alkoxy group inside (structure 42) is favored by 0.3 kcal mol<sup>-1</sup> over that with the alkoxy group outside (structure 43). In contrast, Still and Barrish's hydroborations of related systems prefer to have an allylic OH or OR outside (as in structure 45) when the inside position is crowded by either a *cis* substituent or bulky groups on the borane (45). The model (structures 44 and 45), which has ethyl groups in place of the butyl groups present in the experimental cases, predicts a 60 percent preference for the product formed from structure 45 compared to the experimental value of 86 percent (45).



**Asymmetric hydroborations.** Both 3-pinanylborane and di-3-pinanylborane, prepared from the hydroboration of optically active  $\alpha$ -pinene, react with achiral alkenes to give, after oxidation, alcohols

with a significant excess of one enantiomer, as shown in Fig. 1C. Various qualitative models to rationalize the stereoselectivities observed with di-3-pinanylborane have been devised, but there have been no previous attempts to model these reactions quantitatively. Structures 46 and 47 show the computed transition state models for



the formation of (*R*)- and (*S*)-2-butanol upon reaction of 3-pinanylborane [formed from (+)- $\alpha$ -pinene] with *cis*-2-butene. The preferred transition structure conformation, 46, has the smallest group (H) at the chiral center inside, the medium-sized group outside, and the largest group *anti*. The preferred transition structure has the methyls of *cis*-butene away from the pinanyl group on boron and near the hydrogen attached to boron. The best transition structure (47) leading to the minor product is 1.1 kcal mol<sup>-1</sup> higher in energy, since here the *M* and *L* positions are reversed relative to the lowest energy transition structure. The interaction of *L* with the alkene destabilizes this transition structure. For reactions of dipinan-

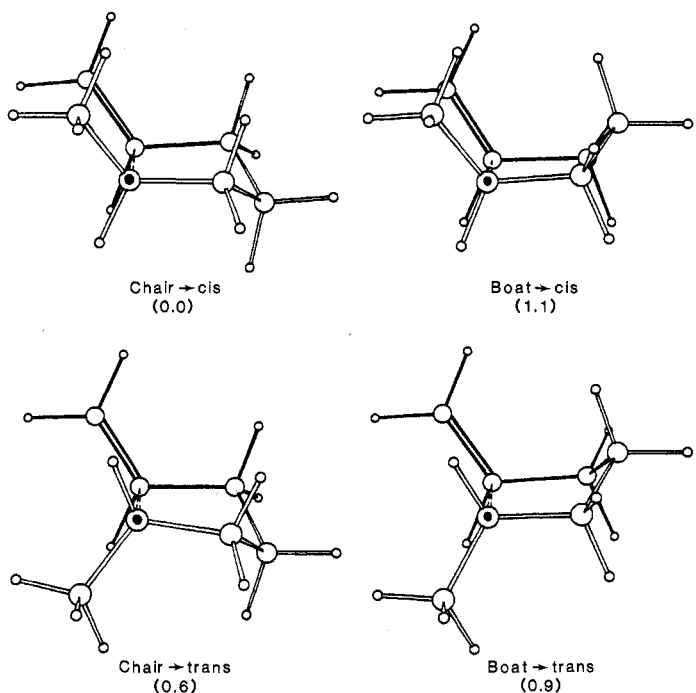


Fig. 6. MM2 models for transition structures of the intramolecular radical additions of the 2-methyl-5-hexenyl radical.

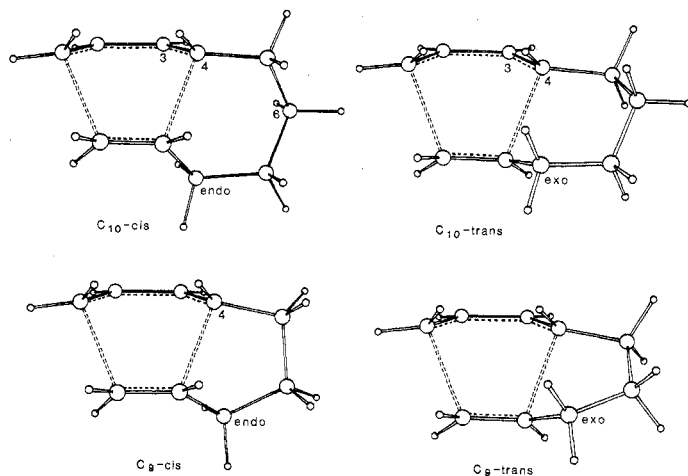


Fig. 7. MM2 models for the intramolecular Diels-Alder reactions of nonatriene and decatriene.

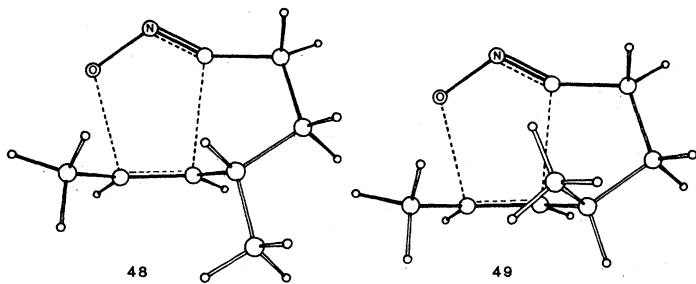
ylborane with *cis*- and *trans*-2-butene, we predict 59 and 68 percent preference, respectively, for formation of the *S* alcohols. Experimental values are 24 and 72 percent (6). For reactions of di-3-pinanylborane with *cis*- and *trans*-2-butenes, we predict 99.8 percent *R* and 19 percent *S*, respectively, whereas these reactions give 98.4 percent *R* and 13 percent *S* (46), the latter through a mechanism involving dissociation of the dipinanylborane. Masamune and co-workers recently have developed some excellent asymmetric hydroborating reagents (47). Our hydroboration model correctly predicted the direction and magnitude of the stereoselectivities observed with the new Masamune reagents (48).

**Intramolecular radical additions.** Beckwith has proposed qualitative models to account for the stereoselectivity in intramolecular radical additions (49); these are finding increasing uses in synthesis. On the basis of *ab initio* calculations on intermolecular alkyl radical additions, we have devised flexible models that parallel experimental observation quite closely. For example, as shown in Fig. 6, the cyclization of the 1-methyl-5-hexenyl radical can give either *cis* or *trans* products via the four transition structures shown. The calculated relative energies of these are shown below each structure. A 39 percent excess of the *cis* adduct is found experimentally (49), whereas the calculations predict a 42 percent excess of the *cis* product. While the Beckwith pseudo-chair model is predicted to be preferred for formation of the *cis* product, the pseudo-boat and pseudo-chair are about the same in energy for the formation of the *trans* product. For reactions of 2-, 3-, and 4-methyl-5-hexenyl radicals, the predicted *cis:trans* ratios of 0.6, 1.9, and 0.4 are close to the experimental ratios of 0.6, 2.5, and 0.2, respectively. In each case, the methyl substituent prefers an equatorial conformation in structures that correspond closely to Beckwith's chairlike model (49) for formation of the major product but a boatlike conformation for formation of the minor product.

**Intramolecular Diels-Alder reactions.** The models for intramolecular Diels-Alder reactions of nonatriene and decatriene are shown in Fig. 7. These are flexible models based on our synchronous STO-3G transition structure for the reaction of butadiene with ethylene (26). The predictions of stereochemistry are only in qualitative agreement with the experimental trends. The 1.0 kcal mol<sup>-1</sup> experimental preference for the *cis* adduct in the nonatriene case is reproduced computationally. The calculations predict a 0.1 kcal mol<sup>-1</sup> preference for the *trans* adduct in the decatriene case (47:53 *cis:trans* at 180°C), whereas a 0.1 kcal mol<sup>-1</sup> preference for *cis* (53:47 *cis:trans*) is found experimentally (50). Nevertheless, these models do explain

the considerable difference in stereoselectivity for these two systems. The *trans* transition structures are destabilized by 1 kcal mol<sup>-1</sup> because of repulsion between the *exo* connecting chain and the *exo* hydrogen at C<sub>4</sub> of the diene. Much of this destabilization is overcome in the decatriene case by the repulsion between the hydrogen at C<sub>3</sub> and the axial hydrogen at C<sub>6</sub> in the *cis* transition structure.

**Intramolecular nitrile oxide cycloadditions.** We have devised a flexible MM2 model for intramolecular nitrile oxide cycloadditions (51) based on the 3-21G fulminic acid-ethylene transition structure. Structures 48 and 49 show the calculated transition structures for one such cycloaddition. Transition state 48 is calculated to be 3.4 kcal mol<sup>-1</sup> more stable than 49. Only the product from 48 is found in this reaction. As pointed out by Kozikowski (51), the repulsion



between the nearby methyls destabilizes structure 49. The corresponding *trans* alkene experiences less destabilization of the transition state related to structure 49, which is now only 0.9 kcal mol<sup>-1</sup> above that related to 48. Here a predicted ratio of 4.6:1 is near the experimental ratio of 3:1. The stereoselectivities of examples substituted at other positions are predicted with greater accuracy.

## Conclusion

The systematic analysis of the steric and electronic factors controlling stereoselectivities has led to general rules for stereoselectivity predictions. There are still many interesting, unanswered questions about electronic and steric effects in transition states, but these may be expected to be answered soon as a result of the ever-expanding availability of computer facilities for the execution of sufficiently high-level calculations.

Quantitative modeling is capable of rationalizing experimental results and providing efficient methods to evaluate the potential of various reagent combinations for highly stereoselective reactions. There are likely to be limitations to the accuracy of these predictions, and force-field models will always be primarily of interpolative and relatively minor extrapolative value. Nevertheless, the perfection of force-field modeling of the type described here will assist the development of rapid and efficient techniques for the synthesis of useful new materials and natural products.

## REFERENCES AND NOTES

- J. D. Morrison and H. S. Mosher, *Asymmetric Organic Reactions* (American Chemical Society, Washington, DC, 1976); J. D. Morrison, Ed., *Asymmetric Synthesis* (Academic Press, New York, 1984), vols. 2 and 3; J. D. Morrison and H. S. Mosher, *Science* **221**, 1013 (1983).
- A stereogenic or chiral center is an atom attached to four different atoms. A chiral molecule is not superimposable on its mirror image. Two molecules that are nonsuperimposable mirror images are called enantiomers. *R* and *S* are designations of the absolute sense of chirality ("right-handed" or "left-handed") of a molecule or of each stereogenic center if there is more than one in the molecule. Diastereomers are stereoisomers that are not enantiomers.
- V. Prelog, *Helv. Chim. Acta* **36**, 308 (1953).
- If a racemic modification is formed (50:50 mixture of the two enantiomers), the reaction is unselective and gives a 0 percent enantiomeric excess (EE). That is, the

- percentage of EE refers to the excess of one enantiomer over the other. For example, a product ratio of 75 percent *R*: 25 percent *S* corresponds to a 50 percent EE of *R*. The definition of diastereomeric excess (DE) is similar when only two diastereomers can be formed in a reaction.
- W. R. Roush, H. R. Gillis, A. J. Ko, *J. Am. Chem. Soc.* **104**, 2269 (1984).
  - H. C. Brown and P. K. Jadhav, in *Asymmetric Synthesis*, J. D. Morrison, Ed. (Academic Press, New York, 1984), vol. 3.
  - K. B. Sharpless et al., *Pure Appl. Chem.* **55**, 589 (1983).
  - E. Ruch and I. Ugi, *Top. Stereochem.* **4**, 99 (1969); L. Salem, *J. Am. Chem. Soc.* **94**, 94 (1973).
  - E. W. Garbisch, Jr., S. M. Schildcrout, D. B. Patterson, C. M. Sprecher, *J. Am. Chem. Soc.* **87**, 2932 (1965); D. F. DeTar and C. J. Tenpes, *ibid.* **98**, 4567 (1976); P. Müller, J. Blanc, J.-C. Perleberger, *Helv. Chim. Acta* **65**, 1418 (1982); W. C. Still and I. Galynker, *J. Am. Chem. Soc.* **104**, 1774 (1982); D. W. Moreland and W. G. Dauben, *ibid.* **107**, 2264 (1985).
  - D. H. R. Barton, *Experientia* **6**, 316 (1950).
  - Pioneering ab initio calculations on models for transition states for asymmetric nucleophilic additions provided the first theoretical evidence for the difference between ground- and transition-state conformations [N. T. Anh and O. Eisenstein, *Nouv. J. Chim.* **1**, 61 (1977)].
  - The difference between the free energies of activation for two reactions determines the ratio of products, according to the following equation:  $\Delta\Delta G^\ddagger = -RT \ln X/Y$ , where  $X/Y$  is the ratio of products, which is equal to  $(100 + EE)/(100 - EE)$ . Because of this logarithmic dependence, less accuracy is needed to predict high stereoselectivity correctly than to predict low stereoselectivity. For example, a prediction that  $\Delta\Delta G^\ddagger = 0 \pm 0.2$  kcal mol<sup>-1</sup> means that the reaction will proceed with  $0 \pm 20$  percent EE at 25°, and a prediction that  $\Delta\Delta G^\ddagger = 2.5 \pm 0.2$  kcal mol<sup>-1</sup> means that a reaction will proceed with  $97 \pm 1$  percent EE.
  - F. M. Menger [*Tetrahedron* **39**, 1013 (1983)] provides a recent review; C. L. Liotta, E. M. Burgess, W. H. Eberhardt, *J. Am. Chem. Soc.* **106**, 4849 (1984).
  - H. B. Burgi, J. M. Lehn, G. Wipf, *J. Am. Chem. Soc.* **96**, 1956 (1974).
  - S. Scheiner, W. M. Lipscomb, D. A. Klier, *ibid.* **98**, 4770 (1976).
  - H. B. Burgi, J. D. Dunitz, E. Shefter, *ibid.* **95**, 5065 (1973); J. D. Dunitz, *X-Ray Analysis and the Structure of Organic Molecules* (Cornell Univ. Press, Ithaca, NY, 1979).
  - M. N. Paddon-Row, N. G. Rondan, K. N. Houk, *J. Am. Chem. Soc.* **104**, 7162 (1982).
  - J. S. Binkley et al., GAUSSIAN 80, QCPE 406, Indiana University, Bloomington; J. S. Binkley et al., GAUSSIAN 82, Carnegie-Mellon University, Pittsburgh, PA.
  - R. W. Strozier, P. Caramella, K. N. Houk, *J. Am. Chem. Soc.* **101**, 1340 (1979).
  - S. Nagase and Y. Uchibori, *Tetrahedron Lett.* **23**, 2585 (1982); E. Kaufmann, P. v. R. Schleyer, K. N. Houk, Y.-D. Wu, *J. Am. Chem. Soc.* **107**, 5560 (1985); K. N. Houk, N. G. Rondan, P. v. R. Schleyer, E. Kaufmann, T. Clark, *ibid.*, p. 2821.
  - P. C. Hiberty, T. Yamabe, M. Koizumi, K. Yamashita, A. Tachibana, *J. Am. Chem. Soc.* **106**, 2255 (1984).
  - K. N. Houk, N. G. Rondan, Y.-D. Wu, J. D. Metz, M. N. Paddon-Row, *Tetrahedron* **40**, 2257 (1984).
  - K. N. Houk, N. G. Rondan, J. Mareda, *J. Am. Chem. Soc.* **106**, 4293 (1984); N. G. Rondan and K. N. Houk, *Tetrahedron Lett.* **25**, 5965 (1984).
  - D. C. Spellmeyer, N. G. Rondan, S. Nagase, M. N. Paddon-Row, K. N. Houk, in preparation.
  - H. B. Schlegel, *J. Phys. Chem.* **86**, 4878 (1982).
  - F. K. Brown and K. N. Houk, *Tetrahedron Lett.* **25**, 4609 (1984).
  - K. Fukui, *Acc. Chem. Res.* **4**, 57 (1971); K. N. Houk, *ibid.* **8**, 361 (1975).
  - P. Caramella, N. G. Rondan, M. N. Paddon-Row, K. N. Houk, *J. Am. Chem. Soc.* **103**, 2438 (1981).
  - M. Cherest, H. Felkin, N. Prudent, *Tetrahedron Lett.* (1968), p. 2199; *ibid.*, p. 2201; *ibid.*, p. 2205.
  - K. N. Houk et al., *J. Am. Chem. Soc.* **106**, 3880 (1984).
  - I. Fleming and J. J. Lewis, *J. Chem. Soc. Chem. Commun.* (1985), p. 149.
  - E. Vedejs and C. K. McClure, *J. Am. Chem. Soc.*, in press.
  - D. J. Cram and F. A. Abd Elhafez, *ibid.* **74**, 5828 (1952); *ibid.*, p. 5851.
  - K. N. Houk, H.-Y. Duh, Y.-D. Wu, S. R. Moses, *ibid.*, in press.
  - H.-Y. Duh and K. N. Houk, in preparation.
  - R. Huisgen, P. H. J. Ooms, M. Mingin, N. L. Allinger, *J. Am. Chem. Soc.* **102**, 3951 (1980); R. Huisgen, *Pure Appl. Chem.* **53**, 171 (1981).
  - N. G. Rondan, M. N. Paddon-Row, P. Caramella, J. Mareda, P. H. Mueller, K. N. Houk, *J. Am. Chem. Soc.* **104**, 4974 (1984).
  - For example, the location of each of the transition structures shown in this article required from 100 to 600 VAX 780 hour equivalents. The time required for these calculations is proportional approximately to the fourth power of the number of atomic orbitals in the system of interest. Our calculations were performed mainly on Harris 800 and 1000 minicomputers.
  - U. Burkert and N. L. Allinger, *Molecular Mechanics* (American Chemical Society, Washington, DC, 1982).
  - W. T. Wipke and P. Gund, *J. Am. Chem. Soc.* **98**, 8107 (1976).
  - A. S. Cieplak, *ibid.* **103**, 4540 (1981).
  - M. M. Midland and Y. C. Kwon, *ibid.* **105**, 3725 (1983).
  - J. Mulzer, *Nachr. Chem. Tech. Lab.* **32**, 16 (1984).
  - D. A. Evans, J. Bartroli, T. Godel, *Tetrahedron Lett.* **23**, 4577 (1982).
  - W. C. Still and J. C. Barrish, *J. Am. Chem. Soc.* **105**, 2487 (1983).
  - J. T. Metz, thesis, University of Pittsburgh (1982).
  - S. Masamune, B. Kim, J. S. Petersen, T. Sato, S. J. Veenstra, T. Imai, *J. Am. Chem. Soc.* **107**, 4549 (1985).
  - Y. Li and K. N. Houk, in preparation.
  - A. L. J. Beckwith, *Tetrahedron* **37**, 3073 (1981). More recently, Beckwith has described an MM2 model similar to ours [A. L. J. Beckwith and C. H. Schiesser, *Tetrahedron Lett.* **26**, 373 (1985); *Tetrahedron* **41**, 3925 (1985)].
  - Y.-T. Lin and K. N. Houk, *Tetrahedron Lett.* **26**, 2269 (1985); F. K. Brown and K. N. Houk, *ibid.*, p. 2297.
  - A. P. Kozikowski, *Acc. Chem. Res.* **17**, 410 (1984).
  - Supported by NIH, NSF, the Petroleum Research Fund administered by the American Chemical Society, and the Harris Corporation.